Statistical Analysis of Wind Turbine Inflow and Structural Response Data From the LIST Program

Luke D. Nelson

Lance Manuel

Department of Civil Engineering,
University of Texas at Austin,
Austin, TX 78712

Herbert J. Sutherland

Paul S. Veers

Wind Energy Technology Department,
Sandia National Laboratories,
Albuquerque, NM 87185

The Long-Term Inflow and Structural Test (LIST) program is gathering inflow and structural response data on a modified version of the Micon 65/13 wind turbine at a test site near Bushland, Texas. Data from 491 ten-minute time data records are analyzed here to determine the dependency of fatigue and extreme loads on inflow parameters. Flap and edge bending moment ranges at a blade root are chosen as the structural response variable, z. Various parameters related to the inflow (including, for example, primary parameters such as the mean and standard deviation of the hub-height horizontal wind speed, and secondary parameters such as Reynolds stresses, vertical shear exponent, etc.) are each considered in an inflow parameter vector, x. Time series for the structural response, z, are processed in order to obtain a structural response parameter, y, where in separate statistical studies, y is taken to be either an equivalent fatigue load or an extreme load. This study describes a procedure by which the important "dependencies" of y on the various variables contained in the inflow parameter vector, x, may be determined considering all the available data. These dependencies of y on x are then recomputed using only the data with above-rated mean wind speeds (taken to be approximately 13 m/s). The procedure employed is similar to other studies, but we do not bin the data sets by wind speed since dependencies in one wind speed bin may be different from those in other bins. Also, our procedure, in sharp contrast to previous studies, examines each inflow parameter in the vector, x, in a sequential analysis, rather than by using multivariate regression. Results from the present study suggest that the primary inflow parameters have a small amount of predictive power in establishing fatigue and extreme loads. In addition, large correlations that exist between several of the secondary parameters individually and each of the primary parameters make it difficult for the secondary parameters to provide any additional explanation of turbine response once the primary parameters have been accounted for. [DOI: 10.1115/1.1627831]

Fundamental to the study of site-specific design loads for wind turbines is an understanding of the influence of inflow parameters on such loads. Inflow parameters might include, for example, mean wind speed, turbulence intensity, roughness length, transverse turbulence, and turbulence length scales for each wind component, to name a few.

The Long-Term Inflow and Structural Test (LIST) program managed by Sandia National Laboratories has made available continuous time series of atmospheric inflow conditions and structural response data from a wind turbine in Bushland, Texas (see Sutherland et al. [1] and Berg and Zayas [2]). In previous studies, Sutherland [3,4] employed the LIST data to assess the influence of atmospheric conditions on damage-equivalent fatigue loads [5]. This same data set is employed in the present study. This study determines the dependencies that exist in blade root flap and edge bending moment fatigue and extreme loads on various inflow parameters.

In contrast with past analyses of these data, this study seeks to examine the ability of inflow parameters to explain the response behavior of a turbine sequentially (i.e., considering one inflow parameter at a time), rather than with a multivariate approach. Since there is a well-accepted practice of using the mean and standard deviation of the horizontal wind speed at the hub height to characterize the design environment, the dependence of these two parameters is first extracted from the loads data. Then, the next most influential parameter is identified and extracted. The goal is that such a procedure can provide a measure of which parameters are most likely to add understanding of the site influence on turbine loads in addition to the ones already in use. Also, with this procedure, the need, as in a multivariate regression, for the inflow parameters (independent variables) to be statistically independent is removed.

The LIST Data Set

The LIST turbine is a three-bladed Micon 65/13M wind turbine that is being tested at a USDA site located near Bushland, Texas. The site is representative of most Great Plains commercial sites. For a complete description of the turbine, its instrumentation, and the site, see Sutherland et al. [1] and Berg and Zayas [2]. A short description of the turbine and the measurement campaign is included here.

The LIST Turbine. The Micon 65/13M LIST turbine, see Fig. 1, is a fixed-pitch turbine with a 3-phase 480V asynchronous generator rated at 115kW. The generator operates at 1200 rpm while the blades turn at a fixed 55 rpm. (Note that the standard Micon 65/13 turbine rotates at a fixed 45 rpm). The turbine is fitted with Phoenix 8m blades that are based on Solar Energy Research Institute (SERI)* airfoils. These "SERI" blades are 7.9 m (312 in) long and are equipped with tip brakes.

*SERI is now the National Renewable Energy Laboratory (NREL).

Data. From the LIST program, data were recorded and stored as ten-minute segments. The experiment was monitored using a total of 60 sensors: 19 sensors measure structural response and 34 sensors measure atmospheric conditions. A total of 1998 ten-minute records are available in this data set. This analysis uses a subset of the data, the records with mean wind speeds greater than 7 m/s (comprising 491 ten-minute records). Figure 2 shows a distribution of the records used, classified according to mean horizontal wind speed. Of these records, 63 have mean wind speeds above the rated wind speed of the turbine (taken to be 13 m/s here).

Numerical Analysis

Several authors have examined the influence of inflow parameters on fatigue loads. Fragoulis [6], Glinou and Fragoulis [7], Sutherland et al. [1], and Sutherland [3] have examined the influence of various inflow parameters on equivalent fatigue loads. Kelley [8] has examined the influence of several parameters on the shape of the fatigue spectrum. The present study is one more study aimed at determining the influence of inflow parameters on both equivalent fatigue loads as well as extreme loads. Data from the LIST program are employed in this study.

Structural Response. The structural response, z, is taken directly from the available ten-minute time series records. In this study, this variable, z, will represent the edge or the flap bending moment at the root of a blade. The time series representing z are processed to yield the variable, y, which is chosen to be, in separate statistical analyses, first, the damage-equivalent fatigue root bending moments (Sutherland [3,4]), and next, the maximum or extreme bending moment. The damage-equivalent load is the constant-amplitude load at a specified number of cycles that produces equivalent damage (in this case, 1000 cycles for each 10-minute sample, Sutherland [5]). The extreme load is the largest load amplitude in each 10-minute sample. The purpose of this analysis is to determine the influence of the inflow parameters on damage-equivalent fatigue loads as well as extreme loads.

Inflow Parameters. The atmospheric time series data are processed to form an inflow parameter vector, x, which is used as the independent variable. This vector consists of a primary inflow parameter vector, x_p, and a secondary inflow parameter vector, x_s. The wind turbine community has a widely held practice of using the horizontal mean wind speed at hub height and a measure of turbulence, such as the standard deviation of horizontal wind speed, as the primary factors that influence fatigue and extreme loads. Accordingly, x_p, the primary inflow parameter vector, is defined to consist of the mean (μ) and standard deviation (σ) of horizontal wind speed.

The vector x_s is defined to consist of sixteen secondary inflow wind parameters. Included in this vector are: the vertical wind shear exponent (α), standard deviations of wind speed in the cross-wind and vertical directions (σ_v and σ_w), turbulence kinetic energy (KE), three orthogonal Reynolds stresses ($u'w'$, $u'v'$, and $v'w'$), local friction velocity (U^*), Obukhov length (L), a stability parameter (z/L), the gradient Richardson number (Ri), turbulence length scales in three orthogonal directions (L_u, L_v, and L_w), and the skewness (S_u) and kurtosis (K_u) of horizontal wind speed. Various authors have proposed one or more of these parameters previously. Rohatgi and Nelson [9] summarize descriptions of many of these parameters. Fragoulis [6], Glinou and Fragoulis [7], Kelley and McKenna [10], and Kelley et al. [11] also propose these and other parameters in studying wind turbine loads. Sutherland [3,4] provides a mathematical description for each of these x_s variables.

Equation (1) summarizes the various primary and secondary inflow parameters used in this study:

$$x = \{x_p, x_s\}; \quad x_p = \{\mu, \sigma\};$$

$$x_s = \{\alpha, \sigma_v, \sigma_w, KE, u'w', u'v', v'w', \ldots$$

$$\ldots U^*, L, z/L, Ri, L_u, L_v, L_w, S_u, K_u\} \tag{1}$$

Regression. We next describe an initial bivariate linear regression that is performed on the primary inflow parameter vector, x_p.

$$\hat{y} = A_0 x_p + B_0; \quad y - \hat{y} = \varepsilon_1 \tag{2}$$

From Eq. (2), the initial residual, ε_1, is defined as the difference between the *observed* value, y, of the dependent variable, and the *predicted* value, $\hat{y}$, resulting from a least squares regression on x_p. Variations of the linear model of Eq. (2) were also considered (such as logarithmic models) but they did not improve on the simple linear regression.

After this initial regression is performed, the residual, ε_1, is regressed on a single parameter from the secondary inflow parameter vector, x_s, as shown in Eq. (3). The selection of one particular element of x_s is made based on the correlation coefficient between ε_1 and each element of x_s. The element in x_s that has the highest correlation with ε_1 is chosen as $x_{s,1}$.

$$\varepsilon_1 = A_1 x_{s,1} + B_1 + \varepsilon_2; \quad \ldots \quad \varepsilon_i = A_i x_{s,i} + B_i + \varepsilon_{i+1} \tag{3}$$
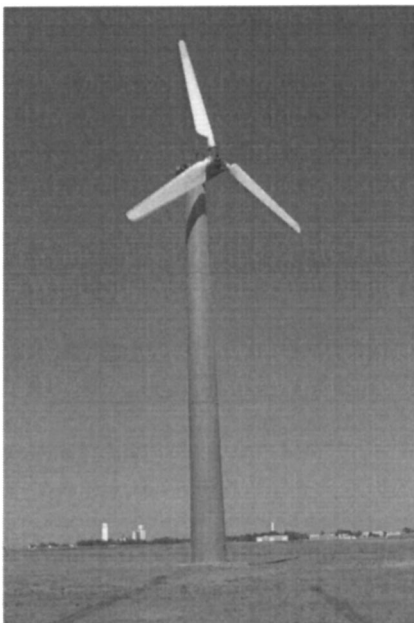

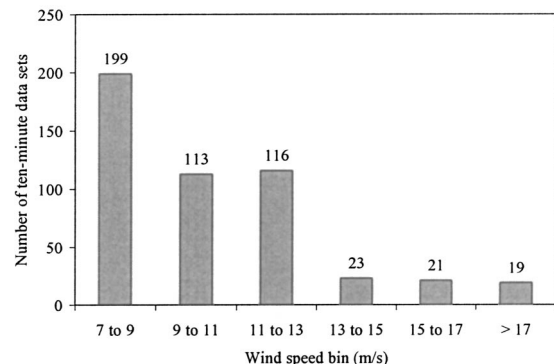**Fig. 1 The LIST Turbine near Bushland, Texas.**

Fig. 2 Distribution of 10-Minute Records Classified by Mean Wind Speed.

Table 1 Statistics of the Inflow Parameters for the Entire Data Set, including Maximum, Minimum, Mean, Standard Deviation, Skewness, and Kurtosis Values.

	μ	σ	α	σ_v	σ_w	KE	$u'w'$	$u'v'$	$v'w'$	U^*	L	z/L	Ri	L_u	L_v	L_w	S_u	K_u
max	18.71	3.14	0.53	3.39	1.32	8.96	0.10	3.22	0.43	1.33	238086.00	239.28	1.93	302.90	324.92	69.11	0.89	4.62
min	7.00	0.28	0.02	0.23	0.05	0.08	−1.76	−2.85	−0.55	0.03	−12297.70	−90.06	−0.48	7.89	2.11	2.31	−1.49	−1.35
mean	10.34	1.41	0.18	1.20	0.76	2.58	−0.39	−0.01	0.00	0.58	-	-	0.16	73.47	55.82	16.26	−0.11	−0.07
std	2.69	0.57	0.10	0.57	0.25	1.87	0.29	0.68	0.11	0.23	-	-	0.27	49.48	55.00	10.89	0.34	0.54
skew	1.20	0.37	1.27	0.77	−0.21	0.86	−1.19	−0.27	−0.54	0.20	-	-	2.06	1.16	1.42	1.25	−0.45	2.74
kurt	4.11	2.63	4.48	3.35	2.56	3.10	4.93	7.85	7.71	2.77	-	-	9.54	4.52	5.12	5.00	4.30	18.88

$$\theta_i = 1 - SE_i/SE_{i-1}; \quad SE_i = \sum_{j=1}^{N} (\varepsilon_i^2)_j \quad \text{for } i \geq 2 \qquad (4)$$

where $(\varepsilon_i^2)_j$ represents the squared residual from data set j of the N sets (note, N is equal to 491 when all the LIST data sets are used) after the ith regression. Only linear models were considered for regression of the residuals on the secondary inflow parameters.

Equation (3) shows how the residual, ε_i, from any step i during this procedure of regression on one element of x_s (indicated here by $x_{s,i}$) leads to a new residual, ε_{i+1}, and the regression procedure continues. The degree of influence that any variable, $x_{s,i}$, has on the amplitude of y is indicated by the parameter, θ_i, in Eq. (4) since θ_i quantifies the reduction in the sum of the squared residuals in step i (relative to step i-1). Thus, a small value of θ_i is an indication that there is no significant benefit of the regression on $x_{s,i}$ in influencing or helping explain the response variable, y. Alternatively, a large value of θ_i, indicates that $x_{s,i}$ does help in predicting or explaining y better. After the initial regression on $x_{s,1}$, the order of selection of each subsequent element of x_s corresponds to the parameter with the highest correlation coefficient between ε_i and each of the unaccounted for elements of x_s. Thus, after each regression step dealing with the parameter, $x_{s,i}$ in the secondary inflow vector, x_s, a newly computed correlation matrix of ε_{i+1} with the remaining parameters of x_s guides the next choice, $x_{s,i+1}$ and the procedure continues; it is stopped when the value of θ_i approaches zero.

This analysis is in sharp contrast to the analyses performed by Fragoulis [6], Glinou and Fragoulis [7], Sutherland et al. [1], and Sutherland [3]. In particular, a sequential analysis is presented here, while the other studies use a single multivariate regression to determine the influence of all the inflow parameters simultaneously. The current procedure takes into consideration correlation among the secondary inflow parameters while the referenced studies do not. The fact that the proposed procedure is sequential is a significant point; one secondary inflow parameter at a time is considered in the regression procedure, rather than simply including all parameters in regression simultaneously as has been done previously. In addition, though, the dependence of loads on inflow parameters is not studied separately for each wind speed bin since previous studies have not been able to explain the widely contrasting findings for each bin that were often observed. Finally, examining the correlation between residuals after each stage of the regression with the inflow parameters not yet considered up to that point in a logical manner (i.e., selecting that parameter that shows largest correlation) ensures that with a reasonably small number of inflow parameters all that can be predicted statistically about the loads may be done. Inflow parameters that do not get included are either not important or are highly correlated with ones that do get included in the regression model.

Data Analysis

Dependent Variables

Fatigue Loads. The blade root fatigue loads for the flap- and edge-wise bending moment are each considered separately as the dependent variable, y. These are characterized using the damage-equivalent fatigue load (see Sutherland et al. [1], Sutherland [3])

and are determined for two fatigue exponents, m, equal to 3 and 10. The former yields an equivalent fatigue load appropriate for welded steel and the latter for fiberglass composites.

In summary, regression analyses were carried out where y, given by Eq. (2), represented four different variables corresponding to damage-equivalent root edge or flap bending moments for m equal to 3 or 10.

Extreme Loads. The extreme blade root flap- and edge-wise bending moments are next considered as the dependent variable, y. The maximum or extreme load is another measure of the severity of a load spectrum. For this analysis, the single largest maximum flap- and edge-wise bending moment value determined from each ten-minute time series was employed.

In summary, regression analyses were carried out where y, given by Eq. (2), represented two different variables corresponding to extreme root edge or flap bending moments.

Numerical Studies. The regression procedure outlined above and described by Eqs. (1–4) was employed for the analysis of several different response time series.

First, the entire available data set of 491 10-minute data segments was used to study the dependencies of flap and edge bending moment fatigue (damage-equivalent) loads for m equal to 3 and 10 on the various inflow parameters in x_p and x_s. The dependency of flap and edge extreme loads on the inflow parameters was also examined for this data set.

Next, similar analyses were performed on a reduced data set consisting of only those 10-minute data segments with a mean horizontal wind speed greater than the rated wind speed (taken to be 13 m/s). Only 63 of the 491 10-minute records were retained in this set of studies that was carried out to compare and contrast the dependency of each response variable, y, on the vector of inflow parameters, x, for the entire data set with that for the reduced (above-rated) data sets.

Statistics for the inflow parameters are presented in Table 1 (for the entire data set) and in Table 2 (for the reduced data set) that summarize sample maximum, minimum, mean, standard deviation, skewness, and kurtosis values. For two of the secondary parameters, L and z/L, the highly variable nature of these parameters makes computing statistical moments meaningless; hence, only maximum and minimum values are presented. Note that for all of the inflow parameters studied, the observed range of all the predictor variables was wide enough to include more than four standard deviations when the entire data set was used, and more than three standard deviations when the reduced data set was used. Because of the adequately wide range of values represented for each of these inflow (predictor) variables in the data sets studied, we believe that the results presented below that lead to conclusions regarding the influence of the inflow variables on fatigue and extreme loads may be made with a fairly high level of confidence (at least for this wind turbine and the data set analyzed).

The selection of mean wind speed and standard deviation of wind speed as "primary" inflow parameters was confirmed as being the most appropriate since we found that the correlation coefficient for each of these two parameters with any choice for variable, y, was larger than that for any of the secondary inflow parameters in the vector, x_s.

Table 2 Statistics of the Inflow Parameters for the Reduced Data Set, including Maximum, Minimum, Mean, Standard Deviation, Skewness, and Kurtosis Values.

|	μ	σ	α	σ_v	σ_w	KE	$u'w'$	$u'v'$	$v'w'$	U^*	L	z/L	Ri	L_u	L_v	L_w	S_u	K_u
max	18.71	3.14	0.21	3.39	1.32	8.96	−0.25	1.84	0.31	1.22	985.63	0.05	0.20	221.92	324.92	49.59	0.71	0.88
min	13.01	1.19	0.09	1.07	0.84	1.87	−1.48	−2.37	−0.35	0.50	−12297.70	−0.55	0.00	56.03	16.06	9.52	−0.64	−0.88
mean	15.86	2.12	0.13	1.93	1.08	4.95	−0.79	0.01	−0.01	0.88	-	-	0.09	122.66	113.86	23.99	−0.07	−0.27
std	1.82	0.44	0.02	0.51	0.12	1.76	0.26	0.77	0.14	0.15	-	-	0.04	42.61	66.07	8.96	0.28	0.34
skew	−0.06	0.07	0.74	0.52	−0.16	0.12	−0.39	−0.55	0.15	−0.19	-	-	0.51	0.32	1.01	1.01	0.33	1.45
kurt	1.66	2.42	4.96	3.03	2.15	2.20	3.45	4.12	2.76	3.22	-	-	2.55	2.33	3.89	3.73	2.95	5.57

Results

The Entire Data Set. The subset of the LIST data used for this analysis contained 491 10-minute data records. Each of these records had a mean wind speed that was greater than 7 m/s.

Fatigue Loads. Figures 3a–3d show results from the bivariate regression of the equivalent fatigue load portion of y performed on the primary inflow parameter vector, x_p. Figures 3a and 3b are for the fatigue damage-equivalent edge bending moments for m equal to 3 and 10, respectively. Similarly, Figs. 3c and 3d are for the damage-equivalent flap bending moments for m equal to 3 and 10, respectively. The regression plane is not shown; instead, the data are shown along with a plot of y versus the mean horizontal wind speed. To represent a range of typical values for the other primary inflow parameter, namely the standard deviation of the horizontal wind speed, σ (denoted as sigma in the figures), three lines based on the regression results and representing sigma values of 1.0, 1.5, and 2.0 m/s are also shown. These three lines are almost coincident, indicating that dependence of the fatigue loads on the standard deviation of the wind speed (sigma) is relatively small for all of these cases.

Table 3 shows correlation coefficients for the residual, ε_1 (see Eq. (3)), with elements of the secondary inflow vector, x_s, after regression of y (in this case, damage-equivalent fatigue loads in the edge and flap bending modes for m equal to 3 and 10) on x_p. The low correlation coefficients indicate that performing further regressions on x_s will not significantly reduce the residuals compared to what was already achieved after regression of y on x_p. To illustrate this, Table 4 shows the results of five additional regressions of residuals, ε_i, performed on one parameter of x_s at a time. Results are shown for all four cases described above (namely, fatigue damage-equivalent edge and flap bending moments with fatigue exponent, m equal to 3 and 10).

As defined earlier, the θ_i term in general describes how much of the variance in residuals is explained by the regression. Note that θ_0 is equivalent to the coefficient of determination, R^2, after the
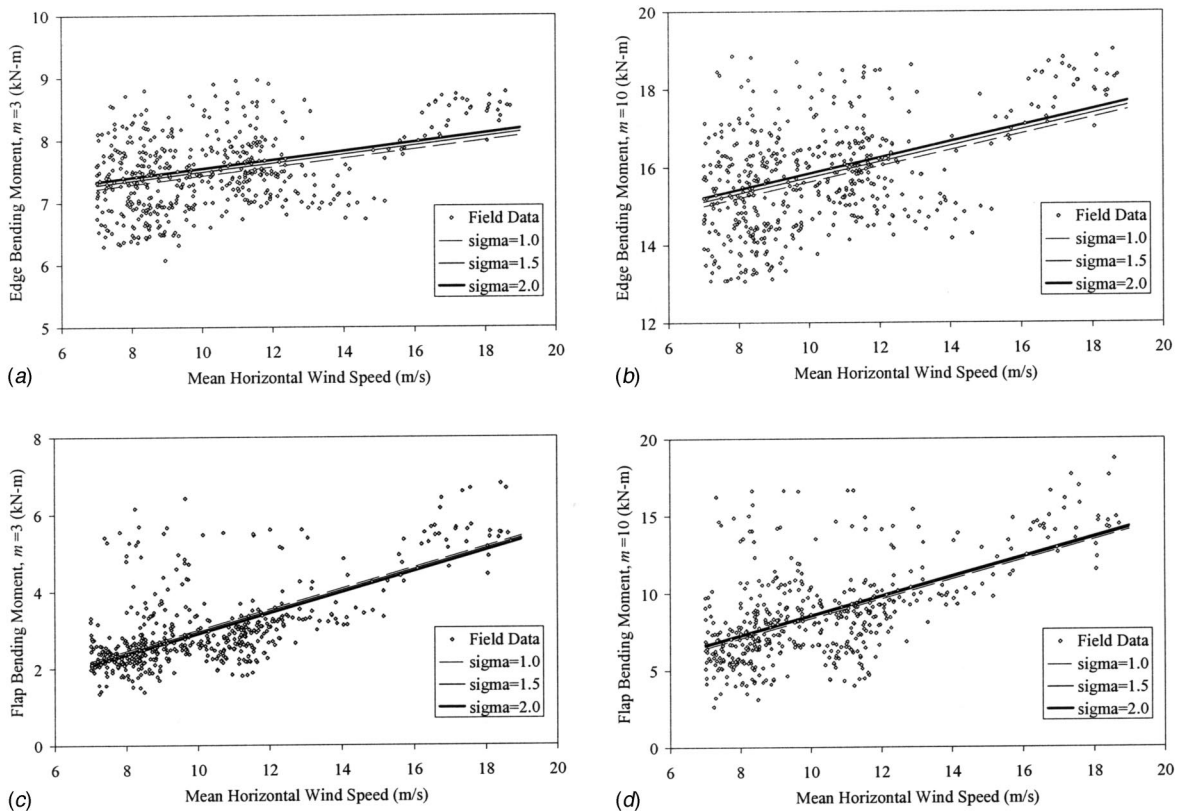
Fig. 3 (a) Equivalent Fatigue Edge BM, $m=3$ versus Wind Speed for the Entire Data Set. (b) Equivalent Fatigue Edge BM, $m=10$ versus Wind Speed for the Entire Data Set. (c) Equivalent Fatigue Flap BM, $m=3$ versus Wind Speed for the Entire Data Set. (d) Equivalent Fatigue Flap BM, $m=10$ versus Wind Speed for the Entire Data Set.

Table 3 Correlation Coefficient Matrix for Damage-Equivalent Fatigue Loads using the Entire Data Set.

		Edge		Flap	
i	$x_{s,i}$	$m=3$	$m=10$	$m=3$	$m=10$
1	α	0.10	0.11	0.10	0.05
2	σ_v	0.05	0.04	−0.03	−0.05
3	σ_w	−0.01	−0.01	−0.04	−0.04
4	KE	0.06	0.05	0.02	0.00
5	$u'w'$	0.01	0.00	−0.02	0.00
6	$u'v'$	0.00	0.00	0.03	0.07
7	$v'w'$	0.06	0.04	−0.03	−0.03
8	$U*$	−0.03	−0.03	−0.01	−0.03
9	L	−0.02	−0.01	0.02	0.02
10	z/L	0.07	0.05	−0.04	−0.06
11	Ri	−0.10	−0.11	−0.04	−0.03
12	L_u	0.02	0.03	0.00	0.02
13	L_v	0.05	0.04	−0.05	−0.06
14	L_w	0.04	0.03	−0.08	−0.07
15	S_u	0.08	0.10	0.13	0.02
16	K_u	0.05	0.03	−0.05	0.00

Table 4 Regression Results for Damage-Equivalent Fatigue Loads using the Entire Data Set.

(a) Edge Bending Moment, $m=3$.

i	x	A_i	B_i	θ_i
0	x_p	[0.07, 0.12]	6.60	0.166
1	α	0.566	−0.100	0.010
2	KE	0.036	−0.094	0.016
3	Ri	−0.179	0.029	0.008
4	K_u	0.064	0.004	0.004
5	S_u	0.135	0.015	0.008

(b) Edge Bending Moment, $m=10$.

i	x	A_i	B_i	θ_i
0	x_p	[0.21, 0.22]	13.35	0.232
1	α	1.327	−0.235	0.012
2	KE	0.076	−0.196	0.015
3	Ri	−0.395	0.064	0.009
4	S_u	0.270	0.031	0.006
5	K_u	0.153	0.010	0.005

(c) Flap Bending Moment, $m=3$.

i	x	A_i	B_i	θ_i
0	x_p	[0.27, −0.10]	0.40	0.409
1	S_u	0.317	0.036	0.017
2	L_w	−0.007	0.111	0.008
3	KE	0.033	−0.085	0.006
4	α	0.652	−0.115	0.006
5	L_u	0.001	−0.068	0.003

(d) Flap Bending Moment, $m=10$.

i	x	A_i	B_i	θ_i
0	x_p	[0.64, 0.23]	1.75	0.356
1	L_w	−0.015	0.244	0.005
2	$u'v'$	0.234	0.003	0.004
3	z/L	−0.009	0.006	0.003
4	L_u	0.003	−0.194	0.003
5	L_v	−0.002	0.115	0.002

first regression. As an illustration, x_p explains anywhere from 17 to 41% of the variance of the residuals, or, equivalently, the regression of y on x_p never leads to R^2 values greater than 0.41. The implication is that y cannot be adequately predicted by the primary inflow parameters, x_p, alone–a fact that can be confirmed by the data shown in Figs. 3a–3d.

Table 4 also shows the sums of squared residuals and the regression coefficients through each step of the procedure. The parameters from x_s shown for i equal to 1-5 in the table are selected based on the highest correlation coefficient of that parameter with the residual from the preceding regression. Thus, for example, for the damage-equivalent edge bending moment with m equal to 3, the parameters of x_s selected are in sequence, α, KE, Ri, K_u, and S_u (the vertical wind shear exponent, turbulent kinetic energy, gradient Richardson number, and the kurtosis and skewness of the horizontal wind speed). It is clear that when the entire data set is used, none of the parameters in x_s has significant influence on reducing the residuals in y in the case of fatigue damage-equivalent bending moments in edge or flap modes. This can be seen by the low values of θ_i for all $i>0$. This also suggests that no secondary inflow parameter usefully contributes to explanation of edge and flap bending fatigue loads once the primary variables of mean wind speed and standard deviation of wind speed are accounted for. Note that we already saw that the R^2 values with the primary inflow parameters alone were very low to begin with. Hence, the finding that the secondary parameters do not contribute additional information suggests that fatigue load levels must de-

pend on some other inflow characteristics (or measures) unaccounted for in the regression models presented here.

Extreme Loads. Figures 4a and 4b show results from the bivariate regression on the extreme load portion of y performed on the primary inflow parameter vector, x_p. Figure 4a is for the extreme edge bending moment while Fig. 4b is for the extreme flap bending moment. Again, the regression plane is not shown; instead, the data are shown along with a plot of y versus the mean horizontal wind speed for three values of the standard deviation of the horizontal wind speed (1.0, 1.5, and 2.0 m/s). For extreme loads, the dependence on the standard deviation of the wind speed
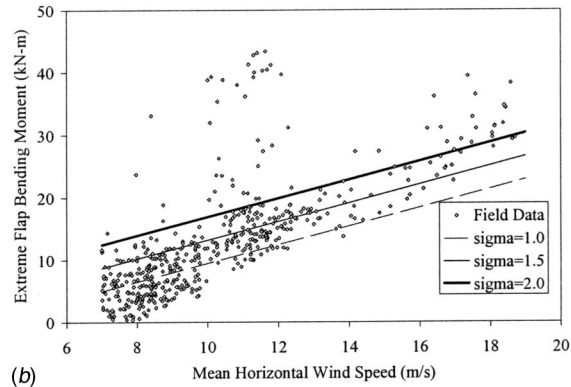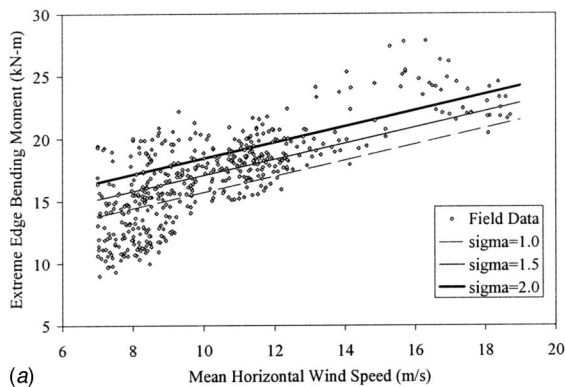
Fig. 4 (*a*) Extreme Edge BM versus Wind Speed for the Entire Data Set. (*b*) Extreme Flap BM versus Wind Speed for the Entire Data Set.

Table 5 Correlation Coefficient Matrix for Extreme Loads using the Entire Data Set.

i	$x_{s,i}$	Edge	Flap
1	α	-0.14	-0.01
2	σ_v	0.11	0.15
3	σ_w	0.10	0.04
4	KE	0.00	0.09
5	$u'w'$	-0.02	-0.04
6	$u'v'$	0.03	-0.01
7	$v'w'$	-0.24	-0.01
8	U^*	0.06	0.05
9	L	0.02	0.01
10	z/L	-0.06	0.05
11	Ri	0.14	0.01
12	L_u	0.09	0.03
13	L_v	0.07	0.14
14	L_w	0.09	0.17
15	S_u	0.16	0.14
16	K_u	0.03	0.02

Table 7 Correlation Coefficient Matrix for Damage-Equivalent Fatigue Loads using the Reduced Data Set.

i	$x_{s,i}$	Edge $m=3$	Edge $m=10$	Flap $m=3$	Flap $m=10$
1	α	0.32	0.27	0.20	0.16
2	σ_v	0.28	0.29	0.30	0.31
3	σ_w	0.23	0.25	0.11	0.12
4	KE	0.19	0.20	0.18	0.20
5	$u'w'$	0.08	0.06	0.13	0.13
6	$u'v'$	0.04	0.10	0.28	0.30
7	$v'w'$	0.14	0.10	0.03	-0.07
8	U^*	-0.08	-0.05	-0.12	-0.13
9	L	0.12	0.11	0.21	0.24
10	z/L	0.13	0.12	-0.04	-0.14
11	Ri	-0.14	-0.11	-0.04	0.03
12	L_u	-0.05	-0.03	-0.05	-0.01
13	L_v	0.05	0.06	0.07	0.17
14	L_w	-0.18	-0.14	-0.14	-0.06
15	S_u	0.21	0.21	0.09	0.10
16	K_u	-0.04	-0.02	-0.07	0.06

is significantly higher than was the case with the fatigue loads. Hence, the three lines shown in Figs. 4a and 4b are well separated.

Table 5 shows correlation coefficients for the residual, ε_1, with elements of the secondary inflow vector, x_s, after regression of y on x_p. The correlation coefficients are still fairly low but higher than for the fatigue loads described earlier. Further regressions on x_s do not significantly reduce the residuals compared to their values after regression of y on x_p as can be seen in Table 6.

In the case of the extreme loads, x_p explains almost 70% of the variance of the residuals (or, equivalently, the regression of y on x_p leads to R^2 values of nearly 0.7 and much better regression fits of y to x_p as may be seen in Figs. 4a and 4b than was the case of the fatigue loads). Table 6 also shows the sums of squared residuals and the regression coefficients through each step of the procedure. Again, as an example, for the extreme flap loads, the parameters of x_s selected are in sequence, L_w, S_u, K_u, α, and σ_v, but it is clear that when the entire data set is used, none of the parameters in x_s has significant influence on reducing the residuals in y in the case of extreme bending moments in edge or flap mode. This can be seen by the low values of θ_i for all $i>0$. This also suggests that no secondary inflow parameter usefully contributes to prediction of edge and flap bending extreme loads.

Reduced Data Set. The subset of the LIST data used for this analysis contained 63 10-minute data records. Only records with mean wind speed greater than 13 m/s are considered.

The purpose for considering this reduced data set is to determine if the dependencies of fatigue and extreme loads on inflow parameters (primary or secondary) might be different in this above-rated wind speed regime compared to the findings based on the use of the entire data set. Some improvement is expected if the above-rated loads represent a more homogeneous data set.

Fatigue Loads. Figures 5a–5d show results from the bivariate regression of the equivalent fatigue load portion of y performed on the primary inflow parameter vector, x_p. Figures 5a and 5b are

Table 6 Regression Results for Extreme Loads using the Entire Data Set.

(a) Extreme Edge Bending Moment.

i	x	A_i	B_i	θ_i
0	x_p	[0.64, 2.72]	6.60	0.695
1	$v'w'$	-4.28	0.00	0.060
2	S_u	0.82	0.09	0.021
3	α	-3.27	0.58	0.028
4	KE	-0.10	0.26	0.010
5	Ri	0.58	-0.09	0.007

(b) Extreme Flap Bending Moment.

i	x	A_i	B_i	θ_i
0	x_p	[1.49, 7.47]	-12.94	0.683
1	L_w	0.08	-1.30	0.029
2	S_u	1.96	0.22	0.017
3	K_u	0.98	0.07	0.011
4	α	3.38	-0.60	0.004
5	σ_v	0.85	-1.02	0.009

Table 8 Regression Results for Damage-Equivalent Fatigue Loads using the Reduced Data Set.

(a) Edge Bending Moment, $m=3$.

i	x	A_i	B_i	θ_i
0	x_p	[0.24, 0.46]	3.14	0.784
1	α	5.11	-0.68	0.100
2	σ_v	0.20	-0.38	0.123
3	U^*	-0.50	0.44	0.080
4	z/L	0.49	0.05	0.031
5	L	0.00	0.02	0.043

(b) Edge Bending Moment, $m=10$.

i	x	A_i	B_i	θ_i
0	x_p	[0.48, 1.36]	6.48	0.790
1	σ_v	0.39	-0.76	0.087
2	α	11.67	-1.56	0.114
3	U^*	-0.97	0.85	0.059
4	L	0.00	0.03	0.025
5	z/L	1.10	0.11	0.030

(c) Flap Bending Moment, $m=3$.

i	x	A_i	B_i	θ_i
0	x_p	[0.36, 0.79]	-2.64	0.707
1	σ_v	0.34	-0.66	0.091
2	$u'v'$	0.21	0.00	0.083
3	$u'w'$	0.51	0.40	0.064
4	α	8.13	-1.09	0.088
5	L	0.00	0.05	0.078

(d) Flap Bending Moment, $m=10$.

i	x	A_i	B_i	θ_i
0	x_p	[0.64, 2.46]	-2.47	0.669
1	σ_v	0.87	-1.67	0.098
2	$u'v'$	0.55	0.00	0.099
3	U^*	-2.20	1.92	0.070
4	α	16.85	-2.26	0.067
5	L	0.00	0.12	0.083

for the fatigue damage-equivalent flap bending moments for m equal to 3 and 10, respectively. The data are shown along with a plot of y versus the mean horizontal wind speed. To represent a range of typical values for the other primary inflow parameter, namely the standard deviation of the horizontal wind speed (sigma), three lines based on the bivariate regression results and representing sigma values of 1.0, 1.5, and 2.0 m/s are also shown. The gradient of bending moment with respect to standard deviation of the wind speed is greater than when the entire data set was used.

Table 7 shows correlation coefficients for the residual, ε_1, with elements of the secondary inflow vector, x_s, after regression of y (in this case, damage-equivalent fatigue loads in the edge and flap bending modes for m equal to 3 and 10) on x_p. The correlation coefficients are higher now when the reduced data set is used as compared to those with the entire data set (see Table 3). This indicates that performing further regressions on x_s might help to reduce the residuals further after the regression of y on x_p. To illustrate this, Table 8 shows the results of five additional regressions of residuals, ε_i, performed on one parameter of x_s at a time. Results are shown for all four cases described above.

With this reduced data set, x_p explains anywhere from 66% to 79% of the variance of the residuals, or, equivalently, the regression of y on x_p leads to R^2 values greater than 0.65. In all cases, y is predicted, to a moderate degree, by the primary inflow parameters, x_p, alone–this can be confirmed by the reasonable fits to the data as seen in Figs. 5a–5d.

For purposes of comparison with the analysis considering the entire data set, for the damage-equivalent edge bending moment with m equal to 3, the parameters of x_s selected are in sequence, α, σ_v, U^*, z/L, and L. It is clear that when the reduced data set is used, at least one or two parameters in x_s have some influence on reducing the residuals in y in the case of fatigue damage-equivalent bending moments in edge or flap mode. This can be seen by values of θ_i greater than 0.10 in a few cases (e.g., with the wind shear exponent, α, in the case of edge-wise fatigue loads). Thus, in a few cases, one or more secondary inflow parameters, in addition to the primary inflow parameters, might contribute to prediction of edge and flap bending fatigue loads, at least relative to the case where the entire data set was used.

In summary, both primary and secondary inflow parameters help to a greater extent in describing fatigue loads when the reduced data set that includes only the above-rated wind speed data is used.

Extreme Loads. Figures 6a and 6b show results from the bivariate regression of the extreme load portion of y performed on the primary inflow parameter vector, x_p. Figure 6a is for the extreme edge bending moment while Fig. 6b is for the extreme flap bending moment. The data are shown along with a plot of y versus the mean horizontal wind speed for three values of the standard deviation of the horizontal wind speed (1.0, 1.5, and 2.0 m/s). Extreme edge loads show little dependence on mean wind speed for this reduced data set, but gradients with respect to standard deviation of wind speed for both edge and flap extreme loads are higher for this reduced data set, as may be confirmed from Figs. 6a and 6b compared to results shown in Figs. 4a and 4b for the entire data set.

Table 9 shows correlation coefficients for the residual, ε_1, with elements of the secondary inflow vector, x_s, after regression of y (in this case, extreme loads in the edge and flap bending modes) on x_p. The correlation coefficients are somewhat higher now when the reduced data set is used as compared to those with the entire data set (see Table 5). They are, however, lower correlation coefficients than were obtained for fatigue loads with this reduced data set (see Table 7). Thus, further regressions on x_s do not
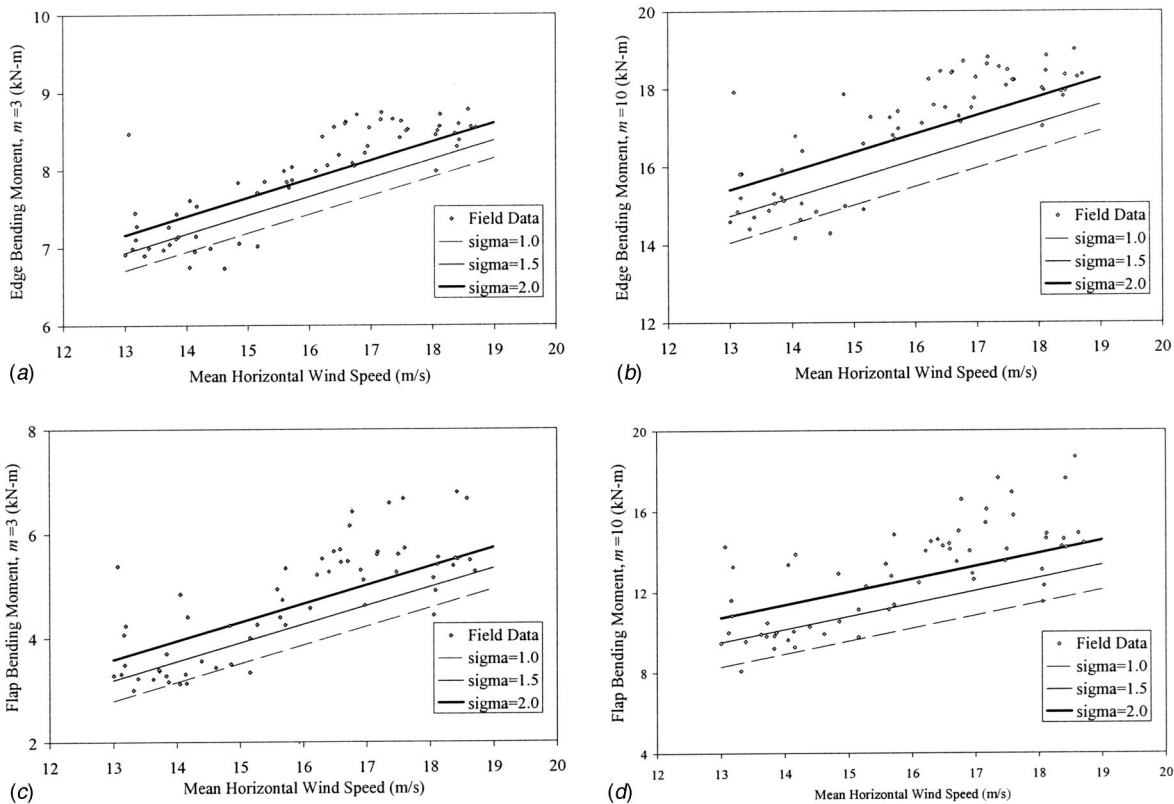

Fig. 5 (*a*) Equivalent Fatigue Edge BM, *m*=3 versus Wind Speed for the Reduced Data Set. (*b*) Equivalent Fatigue Edge BM, *m*=10 versus Wind Speed for the Reduced Data Set. (*c*) Equivalent Fatigue Flap BM, *m*=3 versus Wind Speed for the Reduced Data Set. (*d*) Equivalent Fatigue Flap BM, *m*=10 versus Wind Speed for the Reduced Data Set.

Table 9 Correlation Coefficient Matrix for Extreme Loads using the Reduced Data Set.

i	$x_{s,i}$	Edge	Flap
1	α	-0.17	-0.01
2	σ_v	0.18	0.26
3	σ_w	0.03	0.11
4	KE	0.09	0.17
5	$u'w'$	0.06	0.16
6	$u'v'$	0.03	0.20
7	$v'w'$	-0.02	0.09
8	U^*	-0.05	-0.15
9	L	0.07	0.08
10	z/L	-0.03	-0.16
11	Ri	0.07	0.21
12	L_u	0.11	-0.08
13	L_v	0.00	0.01
14	L_w	-0.04	0.16
15	S_u	0.07	0.16
16	K_u	0.11	-0.01

Table 10 Regression Results for Extreme Loads using the Reduced Data Set.

(a) Extreme Edge Bending Moment.

i	x	A_i	B_i	θ_i
0	x_p	[0.11, 2.77]	-21.95	0.313
1	σ_v	0.72	-1.39	0.032
2	α	-15.48	2.07	0.021
3	L_v	0.00	0.48	0.019
4	K_u	0.79	0.21	0.019
5	$u'v'$	0.15	0.00	0.003

(b) Extreme Flap Bending Moment.

i	x	A_i	B_i	θ_i
0	x_p	[2.23, 5.41]	14.94	0.797
1	σ_v	1.49	-2.87	0.066
2	$u'w'$	2.64	2.08	0.060
3	$u'v'$	0.76	-0.01	0.044
4	L_w	0.06	-1.44	0.039
5	L_u	-0.01	1.51	0.039

Table 11 Correlation Coefficients between the Sixteen Secondary Parameters and the Primary Parameters of Wind Speed Mean (μ) and Standard Deviation (σ).

	α	σ_v	σ_w	KE	$u'w'$	$u'v'$	$v'w'$	U^*	L	z/L	Ri	L_u	L_v	L_w	S_u	K_u
μ	0.33	0.67	0.73	0.64	0.68	0.02	0.03	0.68	0.10	0.02	0.09	0.48	0.52	0.40	0.05	0.14
σ	0.71	0.79	0.87	0.94	0.75	0.03	0.03	0.74	0.09	0.07	0.45	0.64	0.56	0.57	0.05	0.20
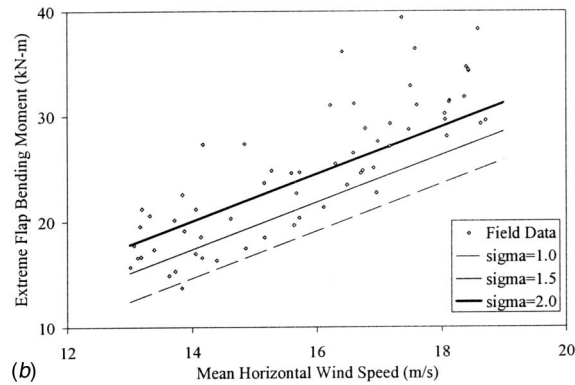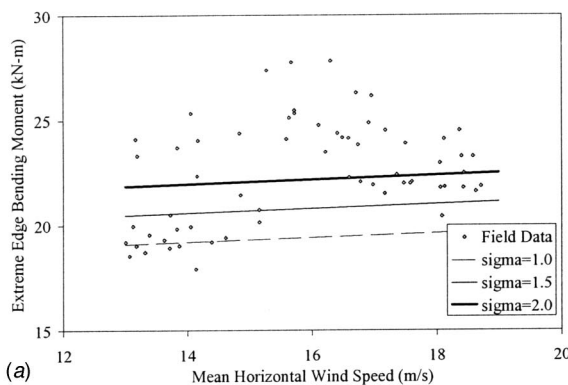
significantly reduce the residuals compared to their values after regression of y on x_p as can be seen in Table 10.

In the case of the extreme loads, x_p explains as much as 80% of the variance of the residuals for the flap bending moment extreme but only 31% for the edge bending moment extreme. This is in contrast to the results when the entire data set was used, where R^2 values of about 70% were computed for both flap and edge extremes. Table 10 also shows the sums of squared residuals and the regression coefficients through each step of the procedure. Again, it is clear that when the reduced data set is used, none of the parameters in x_s has significant influence on reducing the residuals in y in the case of extreme bending moments in edge or flap mode. This can be seen by the low values of θ_i for all $i>0$. This also suggests that no secondary inflow parameter usefully contributes to prediction of edge and flap bending extreme loads after the primary variables of mean wind speed and standard deviation of wind speed are accounted for.

Discussion of Correlation

The degree of correlation among the various primary and secondary inflow parameters makes it difficult to unambiguously identify the most important parameters that influence turbine loads. When one parameter is strongly correlated with another, even though each might be influential to some extent, the first might serve as a surrogate for the second and the importance of the second might be minimized and vice-versa. In this study, after accounting for the first parameter, the influence of the second will have diminished in part due to the strong correlation with the first. Here, we have taken a first step into dealing with issues of correlation by assuming that the mean wind speed and the standard deviation of wind speed will be treated as the "primary" variables of interest. This assumption is based both on design practice and on the physical insight that steady winds in combination with the gross amount of wind fluctuations are reasonable first considerations in the design of wind turbines.

The data set under study suggests that there exists strong correlation between, on the one hand, any one of the two primary inflow parameters, and, on the other hand, one or more of the sixteen secondary inflow parameters. There is also significantly strong correlation among the various secondary parameters. As

Fig. 6 (a) Extreme Edge BM versus Wind Speed for the Reduced Data Set. (b) Extreme Flap BM versus Wind Speed for the Reduced Data Set.

Table 12 Correlation Matrix for the Secondary Inflow Parameters.

	α	σ_v	σ_w	KE	$u'w'$	$u'v'$	$v'w'$	U^*	L	z/L	Ri	L_u	L_v	L_w	S_u	K_u
α	1.00	−0.63	−0.69	−0.65	0.49	0.02	0.02	−0.54	0.02	0.01	−0.65	−0.52	−0.47	−0.57	0.16	0.04
σ_v	−0.63	1.00	0.83	0.90	−0.63	−0.01	−0.03	0.66	0.00	0.03	0.42	0.59	0.76	0.64	0.06	−0.15
σ_w	−0.69	0.83	1.00	0.85	−0.72	0.11	−0.07	0.76	0.02	0.04	0.40	0.51	0.52	0.59	0.00	−0.14
KE	−0.65	0.90	0.85	1.00	−0.73	−0.02	0.03	0.71	−0.01	0.04	0.46	0.61	0.64	0.60	−0.04	−0.17
$u'w'$	0.49	−0.63	−0.72	−0.73	1.00	0.25	0.06	−0.97	−0.03	0.06	−0.21	−0.50	−0.45	−0.55	−0.11	0.24
$u'v'$	0.02	−0.01	0.11	−0.02	0.25	1.00	−0.30	−0.23	0.00	0.01	0.06	0.02	0.00	0.01	−0.16	0.12
$v'w'$	0.02	−0.03	−0.07	0.03	0.06	−0.30	1.00	−0.11	0.01	0.03	−0.08	−0.04	−0.08	−0.08	−0.09	−0.06
U^*	−0.54	0.66	0.76	0.71	−0.97	−0.23	−0.11	1.00	0.04	−0.07	0.26	0.48	0.45	0.56	0.11	−0.25
L	0.02	0.00	0.02	−0.01	−0.03	0.00	0.01	0.04	1.00	0.00	−0.03	−0.03	−0.04	−0.03	0.03	0.00
z/L	0.01	0.03	0.04	0.04	0.06	0.01	0.03	−0.07	0.00	1.00	−0.02	−0.04	0.04	0.09	0.02	−0.05
Ri	−0.65	0.42	0.40	0.46	−0.21	0.06	−0.08	0.26	−0.03	−0.02	1.00	0.33	0.33	0.43	−0.13	−0.07
L_u	−0.52	0.59	0.51	0.61	−0.50	0.02	−0.04	0.48	−0.03	−0.04	0.33	1.00	0.61	0.63	0.00	−0.17
L_v	−0.47	0.76	0.52	0.64	−0.45	0.00	−0.08	0.45	−0.04	0.04	0.33	0.61	1.00	0.59	0.06	−0.12
L_w	−0.57	0.64	0.59	0.60	−0.55	0.01	−0.08	0.56	−0.03	0.09	0.43	0.63	0.59	1.00	0.05	−0.21
S_u	0.16	0.06	0.00	−0.04	−0.11	−0.16	−0.09	0.11	0.03	0.02	−0.13	0.00	0.06	0.05	1.00	−0.38
K_u	0.04	−0.15	−0.14	−0.17	0.24	0.12	−0.06	−0.25	0.00	−0.05	−0.07	−0.17	−0.12	−0.21	−0.38	1.00

seen in Table 11, only about five of the sixteen secondary parameters are relatively uncorrelated with the primary parameters of mean wind speed and standard deviation of wind speed (correlation coefficients less than 0.10). Therefore, each of the other eleven parameters has its relationship with or influence on the response variables largely accounted for by the relationship between the response and the mean and/or standard deviation of the wind speed. Similarly, Table 12, which presents the correlation matrix for secondary inflow parameters, as estimated from the data set, also suggests that several of these parameters are highly correlated with each other, and makes it clear that if a single one of these parameters was represented in the secondary regression scheme outlined, another parameter strongly correlated with it would probably not be represented in subsequent steps in the scheme because, again, its influence would have been mostly accounted for by the strongly correlated secondary parameter already included.

That the secondary parameters contribute so little additional explanation (at most 12% in one particular case and usually much less) implies that there is very little evidence to suggest that they should replace the mean and standard deviation as descriptive parameters. Nevertheless, the fact that one parameter can act as a surrogate for another leaves open the possibility that some secondary parameter may, in fact, be important in driving the magnitude of turbine response.

Conclusions

Data available on inflow and structural response from the LIST program have provided an opportunity to study the influence of various inflow parameters on fatigue and extreme wind turbine loads. A procedure is presented that employed several steps involving regression of loads on primary and secondary inflow parameters. Residuals obtained in each regression step helped in identifying which inflow parameter might be a candidate for regression after more important parameters had already been considered. A systematic approach was followed for damage-equivalent fatigue loads with fatigue exponents of 3 and 10, and for extreme loads representing root flap and edge bending moments.

A reduced data set, including only those ten-minute records with a mean wind speed above the rated wind speed (13 m/s), was employed in an analysis to compare operation above rated (i.e., stalled blades) with the entire data set.

In general, it was found that when the entire data set was used, the fatigue and extreme loads showed few dependencies on either the primary or the secondary inflow parameters. The dependencies were more evident for extreme loads than for fatigue, especially with the primary inflow parameters.

When the reduced data set was employed, the dependencies of loads on primary inflow parameters were found to be greater than when the entire data set was used that included wind speeds lower than rated as well as those above rated. Regression fits on the primary inflow parameters were markedly improved. A few secondary inflow parameters related to wind shear (α) and crosswind variability (σ_v) were identified as somewhat important, especially for fatigue loads.

Results from this study suggest that the large correlation coefficients between several of the secondary parameters individually and each of the primary parameters make it difficult for the secondary parameters to provide any additional explanation of turbine response once the primary parameters have been accounted for.

In summary, the main goal of this study was to employ field data on inflow and response of a wind turbine in order to explain what drives loads of interest when considering failure in either ultimate or fatigue limit states. While primary parameters (mean and standard deviation of the hub-height horizontal wind speed) are traditionally thought of as being important measures of inflow, the extent of their influence on loads is best studied by regression studies such as was done here. Findings from this study were mixed−when the entire data set was considered, linear regression suggested that the primary inflow parameters have limited predictive power. Several secondary inflow parameters also considered did not add useful contributions to predictive power. Conclusions following the use of the reduced data set were somewhat better, at least when measured in terms of regression fits. Overall, though, among the secondary set, no small subset of easily and consistently identified inflow parameters were identified when either fatigue or extreme flap and edge bending loads were considered. This is in contrast to the study by Sutherland [3] where, for fatigue loads, the vertical component of inflow velocity and the Richardson number were identified as having the most influence on loads.

The availability of measurements from the LIST program has offered an opportunity to systematically study the statistical variation of loads with inflow parameters derived from various channels of data gathered. While only the two primary parameters and sixteen secondary parameters that were derived from the data sets available have been considered here, it is likely that much more can be learned about wind turbine loads from measurement campaigns such as the LIST program. Simple inflow statistics as were included here can help to understand loads to a limited extent as this study showed; additional work using the LIST data that includes consideration of spatial coherence of the various inflow data streams can likely help better predict wind turbine loads.

References

[1] Sutherland, H.J., P.L. Jones, and B. Neal, 2001, "The Long-Term Inflow and Structural Test Program," 2001 *ASME Wind Energy Symposium*, AIAA-2001-0039, pp. 1–12.

[2] Berg, D., and J. Zayas, 2001, Accurate Time-Linked Data Acquisition System Field Deployment and Operational Experience, *2001 ASME Wind Energy Symposium*, AIAA/ASME, pp. 153–161.

[3] Sutherland, H.J., 2002, "Analysis of the Structural and Inflow Data from the LIST Turbine," ASME J. Sol. Energy Eng., **124**(4), pp. 432–445.

[4] Sutherland, H.J., 2001, "Preliminary Analysis of the Structural and Inflow Data from the LIST Turbine," *2001 ASME Wind Energy Symposium*, AIAA-2001-0041, pp. 1–12.

[5] Sutherland, H.J., 1999, *On the Fatigue Analysis of Wind Turbines*, SAND99-0089, Sandia National Laboratories, Albuquerque, NM, 132 p.

[6] Fragoulis, A.N., 1997, "The Complex Terrain Wind Environment and Its Effects on the Power Output and Loading of Wind Turbines," *1997 ASME Wind Energy Symposium*, AIAA/ASME, pp. 33–40.

[7] G. Glinou and A. Fragoulis, eds., 1996, *Mounturb Final Report*, 3 vols., JOU2-CT93-0378.

[8] Kelley, N.D., "The Identification of Inflow Fluid Dynamics Parameters that can be Used to Scale Fatigue Loading Spectra of Wind Turbine Structural Components," *1994 ASME Wind Energy Symposium*, ASME, pp. 181–196.

[9] Rohatgi, J.S., and V. Nelson, 1994, *Wind Characteristics, An Analysis for the Generation of Wind Power*, Alternative Energy Institute, Canyon, TX, 237p.

[10] Kelley, N.D., and H.E. McKenna, 1996, "The Evaluation of a Turbulent Loads Characterization System." 1996 ASME Wind Energy Symposium, ASME, pp. 69–77.

[11] Kelley, N.D., A.D. Wright, M.L. Buhl, Jr., and J.L. Tangler, 1997, "Long-Term Simulation of Turbulence-Induced Loads Using the SNL WINd-3D, FAST, YawDyn, and ADAMS Numerical Codes," 1997 ASME Wind Energy Symposium, ASME, pp. 74–85.